The Tertiary DNA Structure in the Single-Stranded hTERT Promoter Fragment Unfolds and Refolds by Parallel Pathways via Cooperative or Sequential Events

Zhongbo Yu,[1] Vanessa Gaerig,[2] Yunxi Cui,[1] HyunJin Kang, [2] Vijay Gokhale, [2] Yuan Zhao,[1] Laurence H. Hurley,[2–4]* Hanbin Mao[1]*

[1]Department of Chemistry and Biochemistry and School of Biomedical Sciences, Kent State University, Kent, OH, 44242

[2]College of Pharmacy, 1703 E. Mabel St., University of Arizona, Tucson, Arizona 85721

[3]Arizona Cancer Center, 1515 N. Campbell Avenue, Tucson, Arizona 85724

[4]BIO5 Institute, 1657 E. Helen Street, Tucson, Arizona 85721

*Corresponding authors: LHH, hurley@pharmacy.arizona.edu (520-626-5622) and HM, hmao@kent.edu (330-672-9380)

Supporting Information
Figure S1 to S10

Figures:

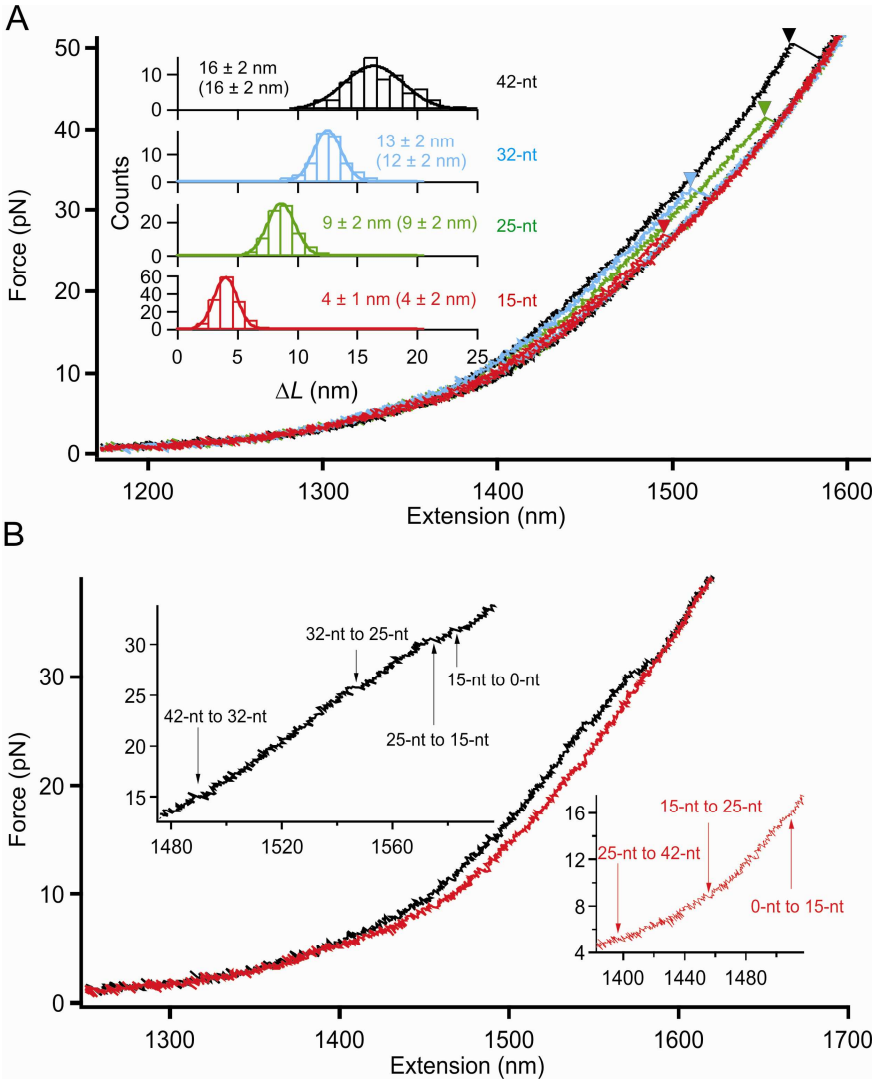

Figure S1. Traditional F-X curves and associated analyses of the change in contour length (ΔL). (a) F-X curves for unfolding transitions of "42"→"0" (black), "32"→"0" (blue), "25"→"0" (green), and "15"→"0" (red) (See Figure 2 in the main text for notation). Insets show ΔL histograms for each transition. Each ΔL value in a histogram was obtained from the analysis of a single F-X curve (see Experimental Section). In comparison, ΔL values obtained from the hysteresis region analysis (Figure 2a in the main text) are shown in parenthesis. (b) A F-X curve depicts the refolding (red) or unfolding (black) transitions involving three intermediates. Top and bottom insets show the blow-up regions that contain unfolding and refolding transitions (depicted by arrows), respectively. As demonstrated here, small transitions are difficult to identify in conventional F-X curves. In contrast, these transitions can be clearly revealed in the hysteresis region analyses (Figures 1d, 2a, and 2b in the main text).

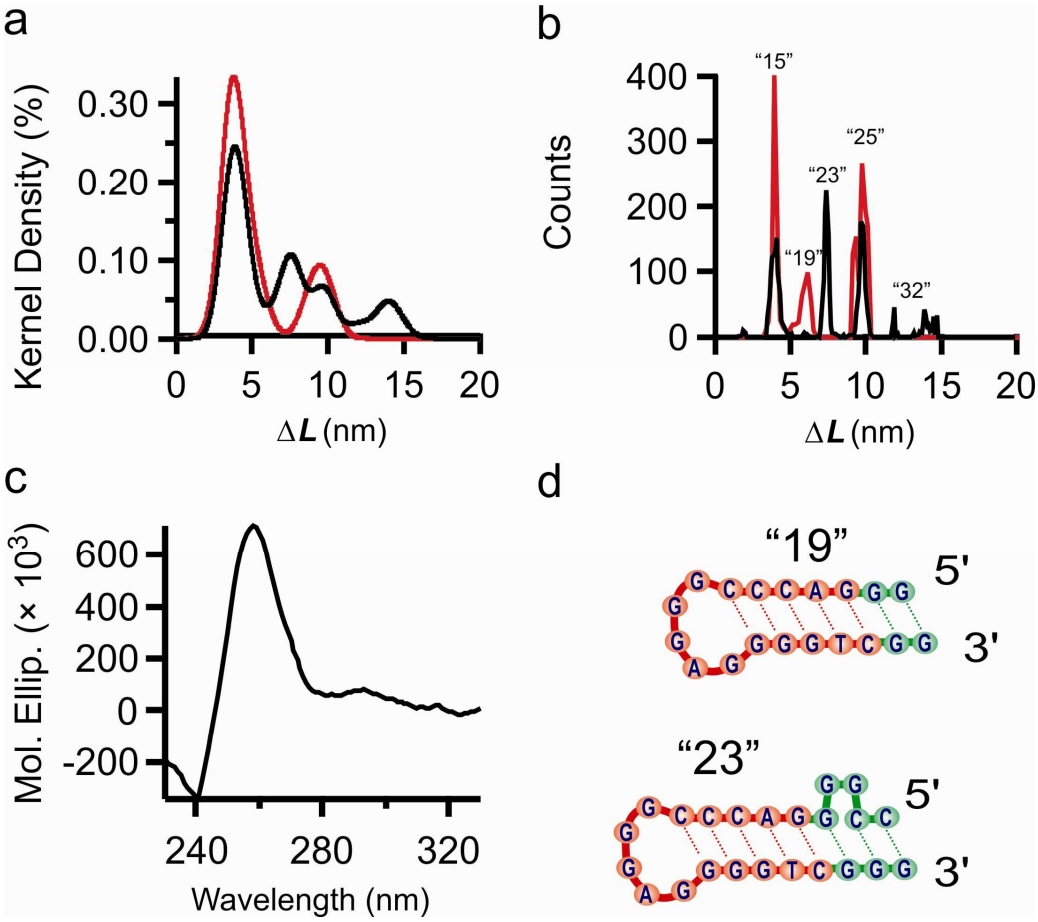

Figure S2. The species formed in the hTERT 5-12 fragment in a 10 mM Tris buffer (pH 7.4) with 100 mM Li^+. (a) Kernel density estimations for ΔL of all transitions (black for the unfolding and red for the refolding process; see Materials and Methods for detailed calculation). (b) Histograms of the ΔL identified by bootstrapping analyses (black for the unfolding and red for the refolding process; see Materials and Methods for detailed calculation). (c) CD spectrum of the hTERT 5-12 fragment in this buffer shows no G-quadruplex formation (see below for CD experiments). (d) Possible conformation for the 19-nt and 23-nt species observed in (b).

In contrast to the 42% formation of the 42-nt (ΔL~16 nm) population in the presence of 100 mM K^+, we did not observe this species in the 10 mM Tris buffer with 100 mM Li^+ (0 out of 45 molecules with a total of 200 F-X curves, see Figure S2a and S2b). This observation was in agreement with the CD measurement (Figure S2c), which showed little G-quadruplex conformation. However, the 15-nt and 25-nt species were clearly observed (Figure S2a and S2b). The 32-nt species can only be poorly determined. This is not surprising because the stand-alone Hoogsteen guanine pairs are relatively weak. Additional species observed under this condition (Figure S2a and S2b) could be ascribed to other hairpin conformations as G-quadruplex structures are inhibited by Li^+ (Figure S2d).

Circular dichroism

Oligonucleotides used for CD measurements were synthesized by Eurofins MWG Operon and were diluted into 5 μM by 10 mM Tris-HCl (pH 7.4) with 100 mM KCl or 100 mM LiCl. Diluted oligonucleotides were annealed by heating at 95 °C for 10 min and cooling to room temperature slowly. CD spectra were recorded on a Jasco-810 spectropolarimeter using a quartz cell with an optical path length of 1 mm in the wavelength range of 230–330 nm, a band width of 2 nm, a scanning speed of 100 nm / min, and a response time of 1 sec at 20 °C.

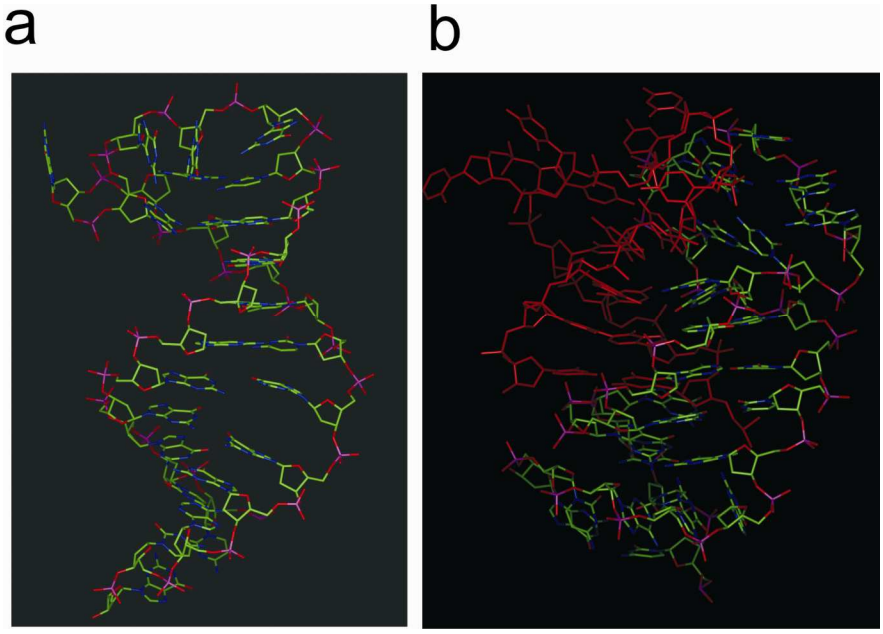

Figure S3. Computer simulation of the "25" intermediate (a) and the interaction between the 15-nt complement (pure red) and the "25" intermediate (b). See Materials and Methods for detailed simulation procedure.

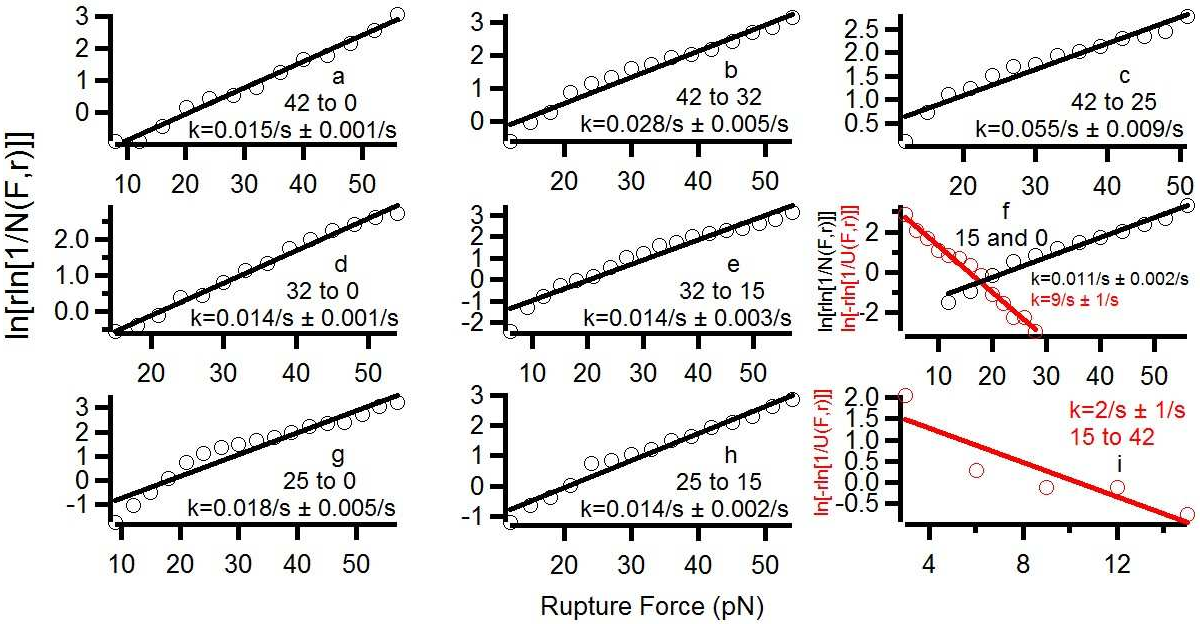

Figure S4. Kinetics calculation (Evans model) for the unfolding (black) and refolding (red) transitions in the absence of the 15-*nt* complementary ssDNA. The numeric number (42, 32, 25, 15, or 0) in each legend represents a specific structure that contains the respective number of deoxynucleotides.

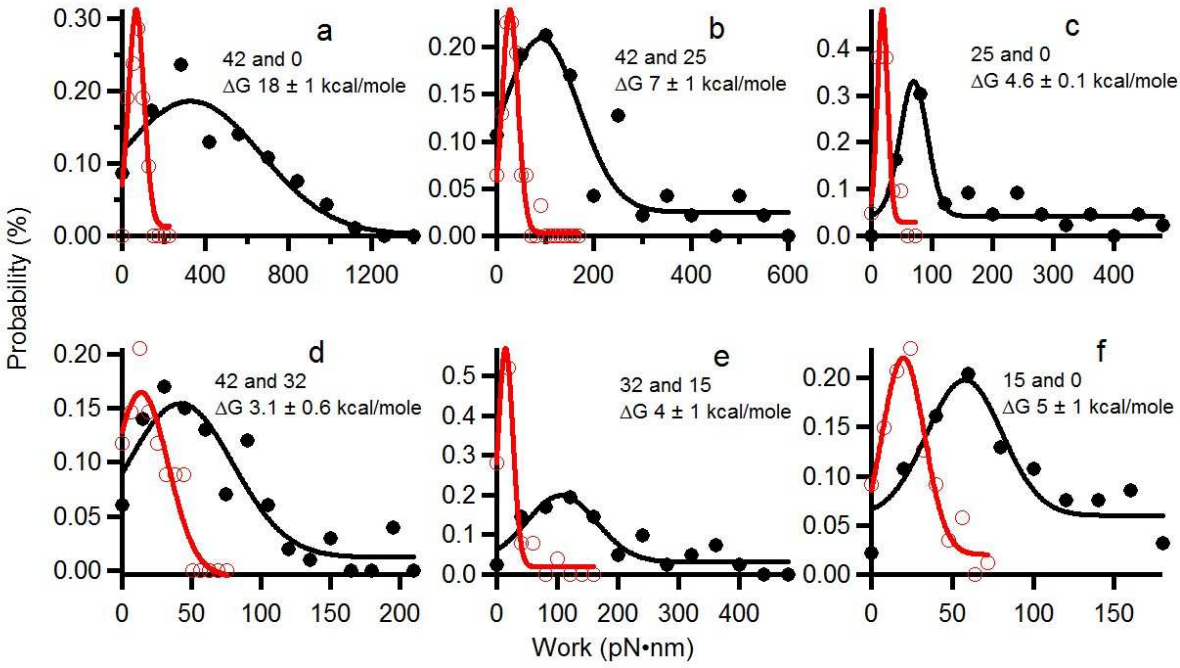

Figure S5. Calculation of change in free energy, Δ*G*, *via* Crook theorem for the transitions in absence of the 15-*nt* ssDNA complement. The work histograms for unfolding (black) and refolding (red) are shown in each diagram. The cross point between the two histograms indicates Δ*G*. The numeric number (42, 32, 25, 15, or 0) in each legend represents a specific structure that contains the respective number of deoxynucleotides.

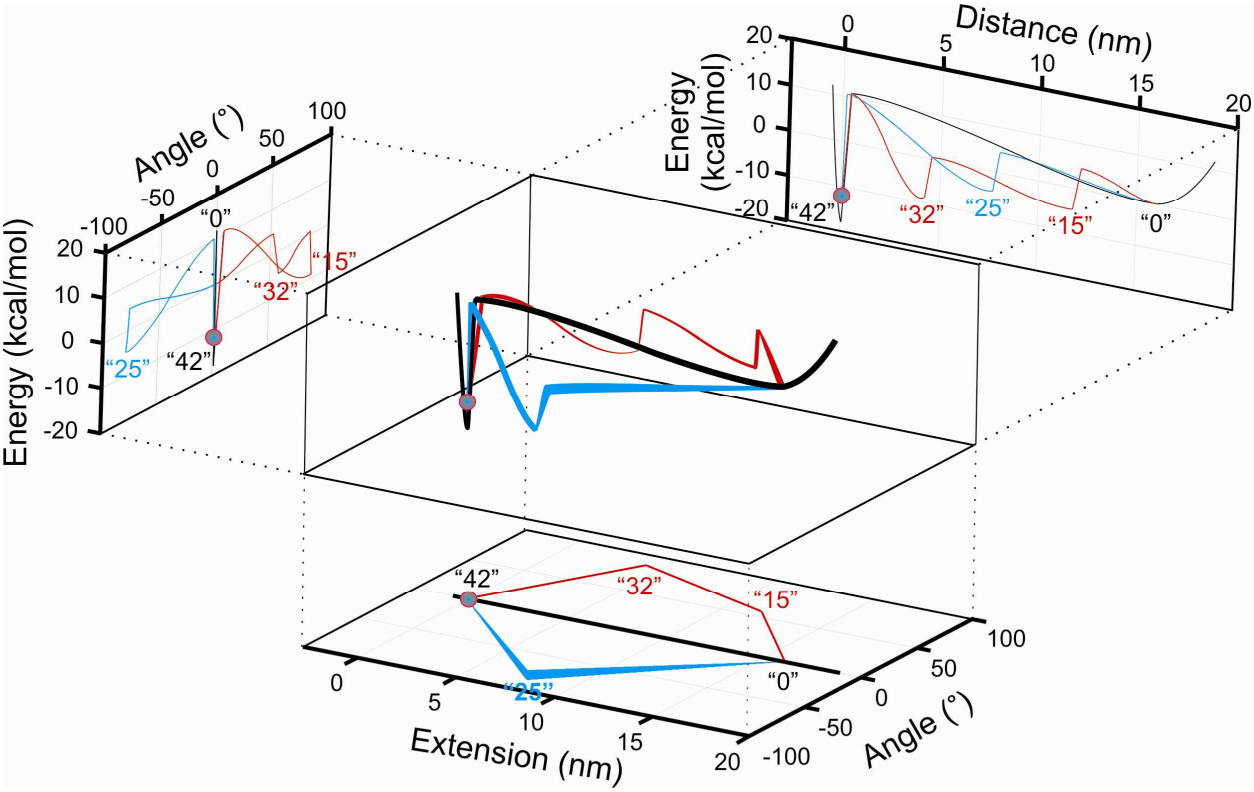

Figure S6. Free energy (kcal/mol) *vs* extension (nm) and angle (°) (see Experimental Section for calculation) for major transitions in the hTERT 5-12 fragment in the absence of the 15-*nt* complementary DNA fragment. Three orthogonal projections are shown. In each diagram, three transitions are shown: "42"→"0" (black), "42"→"25"→"0" (blue), and "42"→"32"→"15"→"0" (red). The colored circle (red circle filled with blue) in each diagram indicates the energy minimum for fully folded structure without tertiary interactions. The bottom of the black energy well (labeled as "42") indicates the fully folded structure with tertiary interactions.

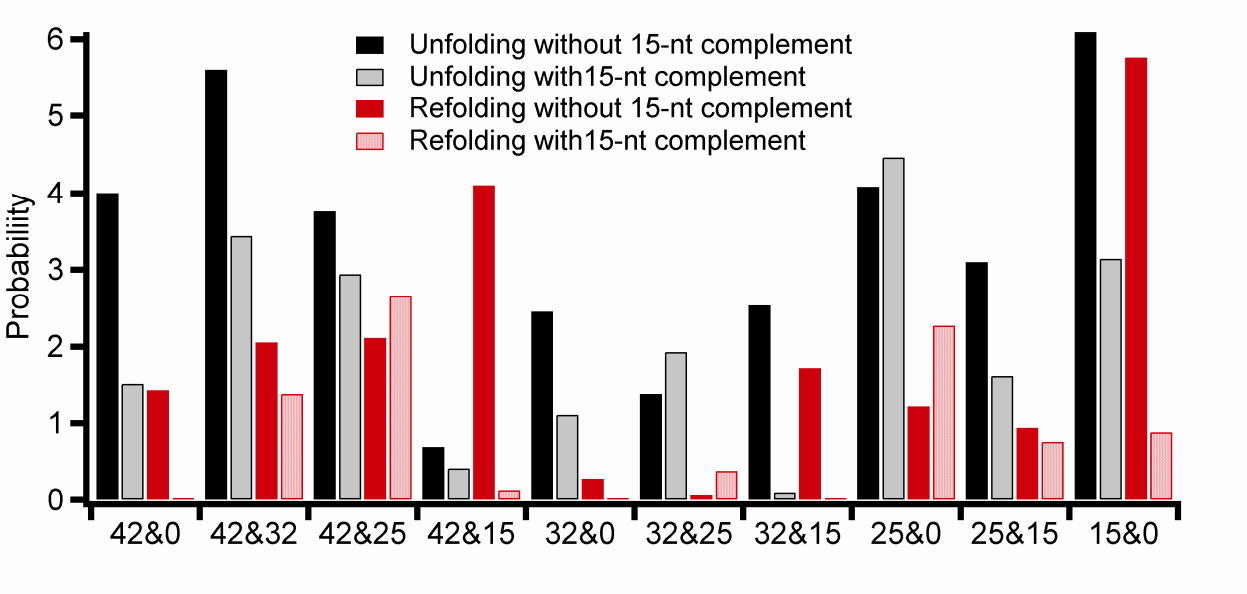

Figure S7. Probability of a specific transition in the hTERT 5-12 fragment. The probability is calculated as the percentage of the occurrence of a specific transition among total number of F-X curves. The numeric number (42, 32, 25, 15, or 0) in *X* axis represents a specific structure that contains the respective number of deoxynucleotides.

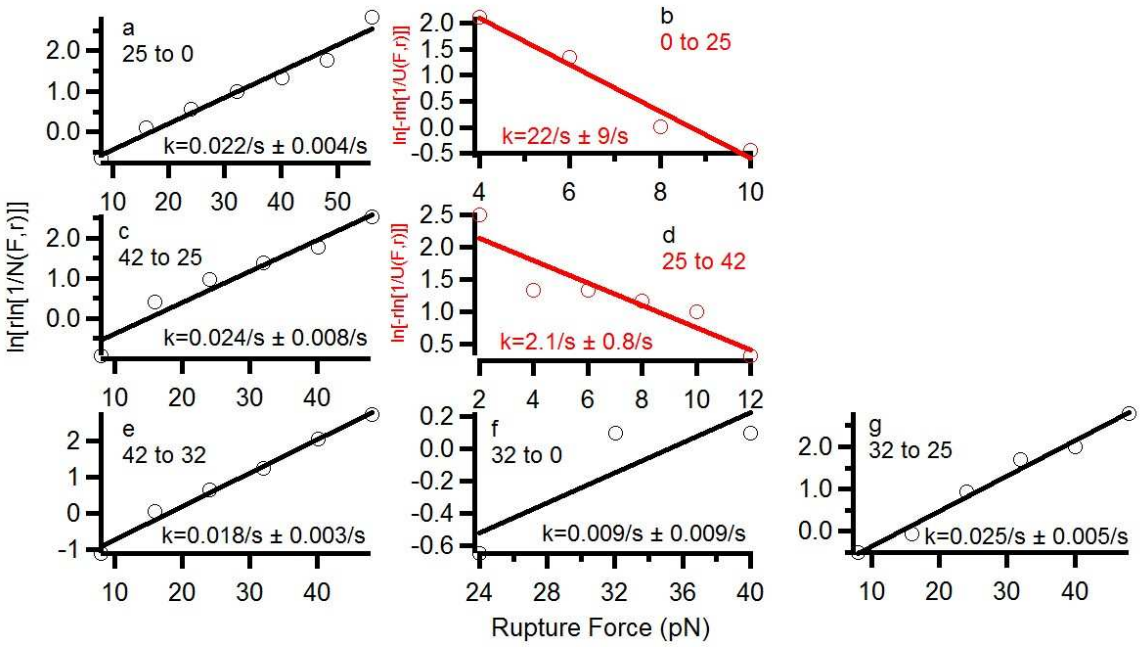

Figure S8. Kinetics calculation (Evans model) for the unfolding (black) and refolding (red) transitions in the presence of the 15-*nt* complementary ssDNA fragment. The numeric number (42, 32, 25, 15, or 0) in each legend represents a specific structure that contains the respective number of deoxynucleotides.

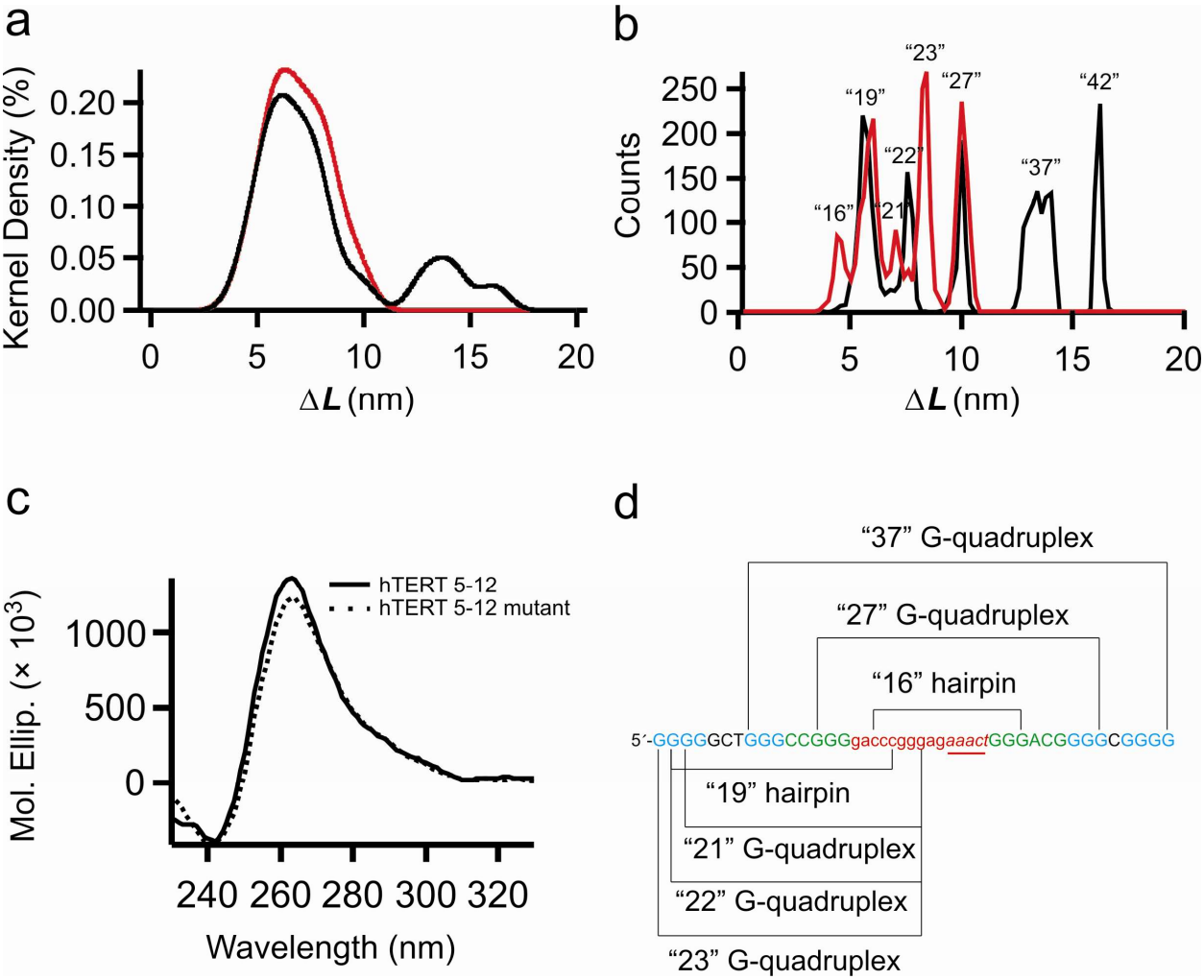

Figure S9. Experiments on the hTERT 5-12 mutant. (a) Kernel density estimations for ΔL of all transitions (black for the unfolding and red for the refolding process, see Materials and Methods for detailed calculation). (b) Histograms of the ΔL identified by the bootstrapping analyses (black for the unfolding and red for the refolding process; see Materials and Methods for detailed calculation). (c) CD spectra (see Figure S2 for details) of the wild type and the mutant hTERT 5-12 fragments in 10 mM Tris (pH 7.4) and 100 mM K^+. (d) The sequence of the mutant with the mutation sites underlined. Due to the destructive effect of the mutation on the fully folded structure (see text), additional populations are observed in (a) and (b). Possible structures that match with the ΔL revealed by the bootstrapping analyses in (b) are labeled.

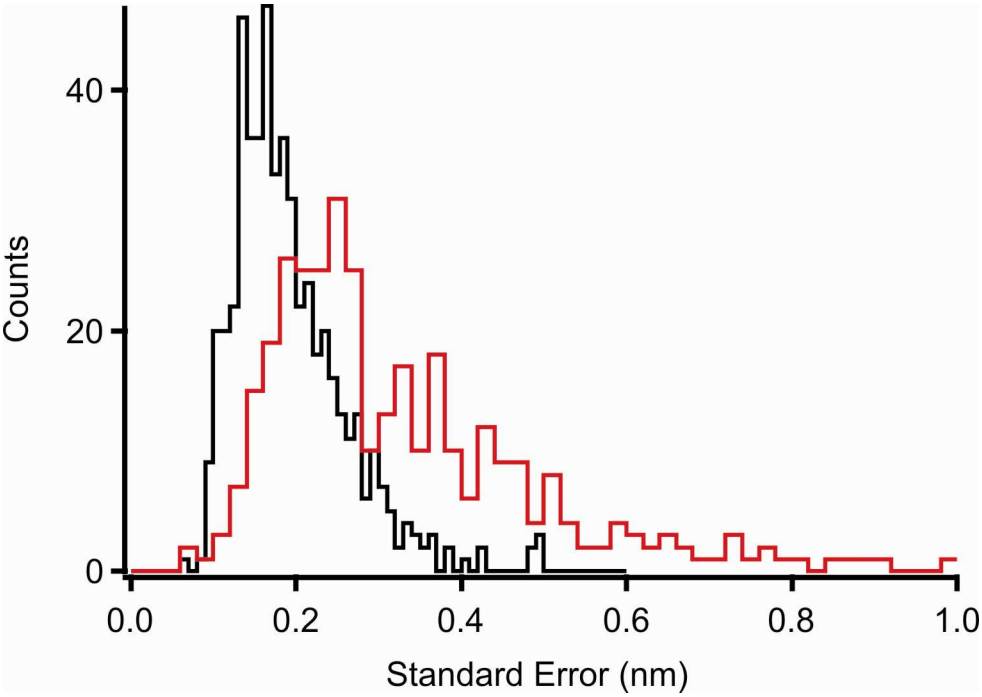

Figure S10. Histograms of the standard error associated with the ΔL measurements (black for the unfolding and red for the refolding process). See Materials and Methods for detailed description.